Logarithmic Terms in Entanglement Entropies of 2D Quantum Critical Points and Shannon Entropies of Spin Chains

Michael P. Zaletel, Jens H. Bardarson, and Joel E. Moore

Phys. Rev. Lett. **107**, 020402 — Published 5 July 2011

DOI: 10.1103/PhysRevLett.107.020402

Logarithmic terms in entanglement entropies of 2D quantum critical points and Shannon entropies of spin chains

Michael P. Zaletel,[1] Jens H. Bardarson,[1,2] and Joel E. Moore[1,2]

[1]*Department of Physics, University of California, Berkeley, California 94720, USA*
[2]*Materials Sciences Division, Lawrence Berkeley National Laboratory, Berkeley, CA 94720, USA*

Universal logarithmic terms in the entanglement entropy appear at quantum critical points (QCPs) in one dimension (1D) and have been predicted in 2D at QCPs described by 2D conformal field theories. The entanglement entropy in a strip geometry at such QCPs can be obtained via the "Shannon entropy" of a 1D spin chain with open boundary conditions. The Shannon entropy of the XXZ chain is found to have a logarithmic term that implies, for the QCP of the square-lattice quantum dimer model, a logarithm with universal coefficient ± 0.25. However, the logarithm in the Shannon entropy of the transverse-field Ising model, which corresponds to entanglement in the 2D Ising conformal QCP, is found to have a singular dependence on replica or Rényi index resulting from flows to different boundary conditions at the entanglement cut.

PACS numbers: 05.30.Rt, 03.67.Mn, 75.10.Pq

The use of quantum information concepts to understand many-particle systems near a quantum critical point (QCP) has grown rapidly since the 1994 calculation of entanglement entropy in one-dimensional (1D) critical systems [1]. Entanglement entropy shows a universal logarithmic divergence at 1D critical points described by 2D conformal field theories (CFTs) [2] and at infinite-randomness 1D critical points [3]. Recent work has studied generalizations to Rényi entropy and the entanglement spectrum [4]. Terms proportional to $\log L$ for a subsystem of size L in an infinite background are especially important as their coefficients are independent of the microscopic lattice spacing and hence potentially universal. Entanglement can be used to develop a classification of 1D interacting quantum systems [5] and determines the difficulty of numerical simulation of 1D QCPs via matrix product state methods [6].

Above one spatial dimension, there are few general results on critical entanglement entropy. For critical points described by a $d+1$-dimensional CFT there is a conjecture for some geometries from the AdS/CFT correspondence [7] for the powers of length that appear in the entanglement entropy: logarithmic terms appear generically only in odd spatial dimensions. This conjecture agrees with 1D results, as well as perturbation theory [8] and variational methods [9] above 1D. For another class of systems, "conformal quantum critical points" (CQCPs) in $d = 2$ [10], whose ground state wavefunctions are related to 2D rather than 3D CFT's, nonperturbative analytical and numerical results are possible and are the focus of the present work. An example of a CQCP is the critical state of the square lattice quantum dimer model [11] originally introduced as a model for high-temperature superconductors.

We investigate logarithmic terms in the von Neumann entropy S and Rényi entropies S_n for CQCPs associated with the compact boson (which has CFT central charge $c = 1$) and the Ising model ($c = 1/2$). One result is the first explicit observation of a universal entanglement entropy logarithm above 1D. For the $c = 1$ boson, the results confirm a conjecture from the initial study of entanglement at CQCPs [12], which derived a formula for a universal, geometry-dependent logarithmic correction to the leading area law. Recent work [13–15] on order-unity ($O(1)$) terms called into question the validity of that formula as for the $O(1)$ terms there are subtle issues related to compactification that took several years and several groups to resolve. We give an improved derivation in supplementary material explaining why subtle factors affecting the $O(1)$ terms are irrelevant for the logarithm.

However, for the Ising CFT we find that the coefficient of the logarithm is discontinuous as the Rényi index n passes through $n = 1$. We explain this behavior analytically by arguing that the correct "defect line" used in the calculation of the entropy changes discontinuously with n and is not the combination of one free field and $n-1$ Dirichlet fields as conjectured in Ref. 12 and confirmed for the boson. A similar but less singular discontinuity in n was previously found numerically to exist for the $O(1)$ term [16]. Our numerical approach to logarithmic terms uses large-scale Time-Evolving Block Decimation (TEBD) [17] calculations to implement the same mapping used there between entanglement entropy at 2D CQCPs and the Shannon entropy of 1D spin chains. The compact boson case relevant to the quantum dimer model seems to be well understood, but the results here demonstrate that the correct defect boundary condition can be complicated and n-dependent.

We first define some basic concepts. The bipartite entanglement spectrum $\{p_\sigma\}$ of a pure quantum state consists of the eigenvalues of the reduced density matrix of either subsystem. The von Neumann entropy S and Rényi entropies S_n are defined by

$$S = -\sum_{\{\sigma\}} p_\sigma \log p_\sigma, \quad S_n = \frac{1}{1-n} \log(\sum_{\{\sigma\}} p_\sigma^n). \qquad (1)$$

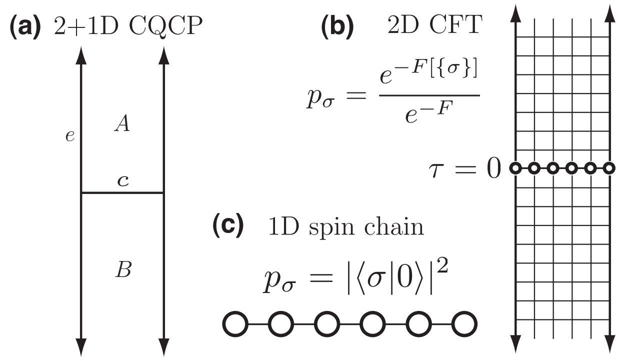

FIG. 1. a) The entanglement spectrum of the CQCP, p_σ, in a strip geometry is in one-to-one correspondence with field configurations $\{\sigma\}$ on the entanglement cut. These probabilities can be alternately understood as b), partition functions for a constrained CFT in the strip geometry, or c), ground state amplitudes of a quantum chain.

The entanglement spectrum $\{p_\sigma\}$ of a CQCP ground state in strip or cylinder geometries can be understood both in terms of the associated 2D CFT or as probability amplitudes of a 1+1D spin chain, as illustrated in Fig. 1. The entanglement spectrum $\{p_\sigma\}$ is in one-to-one correspondence with CFT field configurations $\{\sigma\}$ along the entanglement cut. If the CQCP lies on a strip or cylinder, the 2D CFT naturally defines a 1D quantum Hamiltonian H via the transfer matrix formalism. 'Time' is chosen parallel to the strip (cylinder), with the entanglement cut at a fixed time $\tau = 0$. For universal properties, we can take the spatial direction to lie on a lattice. In the limit of an infinite strip the ground state probabilities are identical to the entanglement spectrum of the associated CQCP [13]. The Shannon entropy of the spin chain, defined as in Eq. (1) with $p_\sigma = |\langle\sigma|0\rangle|^2$, is a basis dependent measure of disorder in the ground state. The Shannon entropy of the spin chain is then equivalent to the bipartite von Neumann entropy of the CQCP.

The relationship between the CQCP entanglement spectrum, spin chain ground state probabilities, and CFT partition function is summarized by

$$p_\sigma = \lim_{\beta\to\infty} \frac{\langle i|\, e^{-\beta H}\,|\sigma\rangle\,\langle\sigma|\, e^{-\beta H}\,|i\rangle}{\langle i|\, e^{-2\beta H}\,|i\rangle} = |\,\langle\sigma\mid 0\rangle\,|^2 \quad (2)$$

$$= \lim_{m\to\infty} \frac{\langle i|\,\mathcal{T}^m\,|\sigma\rangle\,\langle\sigma|\,\mathcal{T}^m\,|i\rangle}{\langle i|\,\mathcal{T}^{2m}\,|i\rangle} = \frac{e^{-F[\{\sigma\}]}}{e^{-F}}\ . \quad (3)$$

Here $\mathcal{T}$ is the transfer matrix of the CFT, and the result is independent of the boundary state $|i\rangle$ in the limit of an infinite strip. With a basis $\{\sigma\}$ for the Shannon entropy, the projection operator $|\sigma\rangle\,\langle\sigma|$ in the numerator of Eq. (3) constrains the corresponding field of the CFT along a cut at $\tau = 0$; the bulk fields remain free. The numerator and denominator are thus constrained and unconstrained partition functions, with free energies $F[\{\sigma\}]$ and F respectively.

The Rényi entropies S_n suggest a thermodynamic notation

$$\mathcal{Z}(n) = e^{-F(n)} \equiv \sum_{\{\sigma\}} p_\sigma^n = \sum_{\{\sigma\}} e^{-n(F[\{\sigma\}]-F)}, \quad (4)$$

defined so that $F(n) = (n-1)S_n$. The 'free energy' $F(n)$ is found to depend on the length of the chain L as

$$F(n, L) = f_1(n)L + \gamma(n)\log(L/a) + f_0(n) + \cdots\ . \quad (5)$$

At a critical point $\gamma(n)$ should be universal and determined by the CFT as it is independent of the UV cutoff $1/a$. In the case of a cylinder geometry, $\gamma(n)$ is zero for an arbitrary CFT as the trace anomaly from a smooth conformal defect line is zero. For a strip geometry, a universal logarithmic term is expected as explained below.

For integer n, $\mathcal{Z}(n)$ can be interpreted as the partition function of a replicated CFT with n copies of the field constrained to agree along $\tau = 0$, normalized by the free partition function. $F(n)$ is then interpreted as the free energy of a defect line in the replicated CFT. If the logarithmic contributions can be calculated in the replicated CFT and analytically continued to $n = 1$, then the entire spectrum of Rényi entropies S_n as well as S is known, via $S = \partial_n F(n)|_{n=1}$. (Below, this 'replica trick' is found to fail for the Ising model due to non-analyticity of $F(n)$ at $n = 1$ in the thermodynamic limit.)

We start with numerical evidence for the existence of logarithmic terms in the case of the $c = 1$ compact boson, the CFT associated with the CQCP of the square-lattice quantum dimer model. For a free boson, Ref. 12 predicted a contribution $-\frac{1}{4}\log(L) \in S$ in the strip geometry; we indeed find a logarithm $-\frac{1}{4}\log(L)$ for the external boundary conditions (on the edge of the strip) assumed there, and for an alternate boundary condition we obtain $+\frac{1}{4}\log(L)$ as derived below. By using the transfer matrix mapping, it is sufficient to calculate the Shannon entropy of a 1D quantum model, the spin-1/2 XXZ chain

$$H = -h(\sigma_1^x + \sigma_L^x) + \sum_{i=1}^{L-1} \left[\sigma_i^x\sigma_{i+1}^x + \sigma_i^y\sigma_{i+1}^y + \Delta\sigma_i^z\sigma_{i+1}^z\right]. \quad (6)$$

In the continuum limit the XXZ model is described by a compact boson. The boundary conditions are tuned by an external field h on the surface sites, and the Shannon entropy is calculated using the σ^z basis.

The ground state was found by TEBD for L $= \{2, 4, \cdots, 30\}$ at $\Delta = \{-\frac{1}{2}, 0, \frac{1}{4}, \frac{1}{2}, \frac{3}{4}\}$. We estimate the ground state error to be of order $\epsilon = 1 - |\,\langle 0\mid\Psi\rangle\,|^2 \sim \mathcal{O}(10^{-6})$, which was verified for the exactly solved $\Delta = 0$ case. The partition function $\mathcal{Z}(n)$ was then computed by summing over all 2^L configurations. The logarithmic contribution $\gamma(n)$ was extracted from the finite-size data as described in Fig. 2a. $\gamma(n)$ is well described by

$$\gamma(n) = \mp\frac{1}{4}(n-1) \quad (7)$$

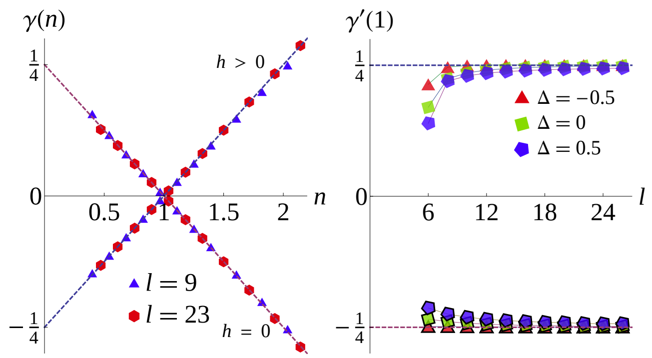

(a) (b)

FIG. 2. a) The logarithmic part of $F(n)$ at $\Delta = -1/2$. Data is included both without ($h = 0$) and with ($h > 0$) an edge magnetic field. $F(n, L)$ was computed for $L = 2, 4, \cdots 30$. Windows of 6 data points centered at ℓ, $L = \{\ell-5, \cdots, \ell+5\}$, were fitted to the form $f_1 L + \gamma \log(L) + f_0 + f_{-1} L^{-1}$. The data displayed includes γ for $\ell = \{9, 23\}$. The approach of $\gamma(n)$ to the dashed lines suggests convergence to $\gamma(n) = \mp\frac{1}{4}(n-1)$ as $\ell \to \infty$, for $h = 0$ and $h > 0$ respectively. The inclusion of a L^{-1} term accelerates convergence, but the value of $\gamma(n)$ remains insensitive to within a few percent to the choice of fitting form for terms that vanish as $L \to \infty$, as discussed in the supplementary material. b) The logarithmic contribution to the von Neumann entropy $S(L)$, as a function of the fitting window center ℓ. As ℓ increases, the logarithm's coefficient converges to $\mp 1/4$, depending on the boundary conditions. Successive lines are for $\Delta = \{-1/2, 0, 1/2\}$.

for $h = 0$ and $h > 0$ boundary conditions respectively. For the compact free boson, Eq. (7) is correct for all n, while for XXZ and dimer lattice realizations, the result is modified in the regime $n \geq 2$ due to additional boundary operators becoming relevant [18].

The slope of $\gamma(n)$ at $n = 1$ is of special interest as the von Neumann entropy is given by $S = \partial_n F(n)|_{n=1}$ if the derivative exists. In the case of the XXZ model, there is a logarithmic contribution $\partial_n \gamma(n)|_{n=1} = \mp\frac{1}{4}$, so the von Neumann entropy scales as

$$S(L) = s_1 \cdot L \mp \frac{1}{4} \log(L/a) + \cdots \quad . \tag{8}$$

The rapid convergence of $S(L)$ to Eq. (8) with increasing L is illustrated in Fig. 2b.

To derive Eq. (7), we perform a Jordan-Wigner transformation on the XXZ spin chain and bosonize the resulting fermionic model. The model is mapped onto the universality class of a free, compact boson ϕ for $|\Delta| < 1$, with a compactification radius R that depends on Δ. For $h = 0$ the external boundary condition (b.c.) is Dirichlet in the continuum limit, $\phi = 0$, while for $h \neq 0$ the external b.c. is Neumann, $\partial_x \phi = 0$ [19]. The resulting change in the logarithmic contribution is thus attributed to 'boundary condition changing operators' (bcc operators) in the underlying CFT. For integer n, the replicated theory contains n copies of the field, ϕ^a, subject to the constraint $\phi^a = \phi^b$ along the $\tau = 0$ cut, modulo compactification. In the analogous problem for a non-compact boson, the action, external b.c.'s, and path integral measure are all invariant under an $O(n)$ rotation of the replica index, so we can rotate the replicated fields to a new basis which includes the 'center of mass' field $\phi_{CM} = \frac{1}{\sqrt{n}} \sum_{a=1}^{n} \phi^a$. The gluing condition now factorizes, giving the free center of mass field plus $(n-1)$ decoupled fields satisfying Dirichlet b.c. on the cut 12. The free energy is

$$F(n) = (n-1)(F_D - F) \tag{9}$$

where F_D is the free energy of a *single* replica with Dirichlet b.c. on the cut and F is the unconstrained free energy. Using this rotation, the logarithmic contribution to $F(n)$ follows from the free energies F_D and F of a single replica.

Logarithmic contributions to the free energy of a CFT arise from a 'trace anomaly,' in which the trace of the stress tensor $\langle T^\mu_\mu \rangle$ does not vanish. In the relevant 'cut strip' geometry, the anomaly arises from the four corners where the cut along $\tau = 0$ terminates into the external boundary, as illustrated in Fig. 1a. The geometry of the corner contributes a term proportional to the central charge c [20]. However, there can also be a contribution due to the changing b.c.: if the external b.c. is Neumann, then termination of the Dirichlet b.c. on the cut into the external Neumann b.c. introduces a bcc operator [21]. The scaling dimension of this bcc operator, h_{ND}, will appear as an extra contribution to the trace anomaly.

For an arbitrary CFT in the 'cut strip' geometry the predicted coefficient of the logarithmic term is

$$L\partial_L(F_c - F) = 2 \times 2 \left[2h_{ec} - \frac{c}{16} \right] . \tag{10}$$

F is the free energy of the strip with no constraint at $\tau = 0$, while F_c is the free energy when constrained to some b.c. 'c' along the cut, and both obey external b.c. 'e'. Here h_{ec} is the scaling dimension of the bcc operator required to take the external b.c. e to the b.c. c on the cut. This result can be extended if e.g. the cut is not perpendicular to the boundary. In the compact boson case, $c = 1$, and the scaling dimension h_{eD} is 0 or 1/16 for $e = D, N$ respectively. Substituting into Eq. (10), $L\partial_L(F_D - F) = \mp\frac{1}{4}$ for D/N respectively, i.e., the sign of the logarithmic term depends on the external b.c. The XXZ results are well described by the rotation trick and this bcc operator effect. It can be shown (supplementary material) that the logarithm is unaffected by compactification, as supported by the XXZ data. Briefly, field configurations can be decomposed into two sectors: fluctuations versus zero modes or vortices. Only the latter, topological sector is affected by compactification. The fluctuating sector can be rotated. The topological sector has exact conformal invariance: the trace anomaly and logarithm arise only from the fluctuations. Hence

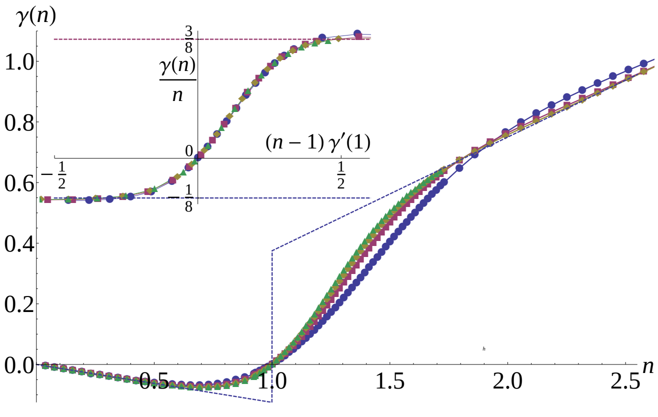

FIG. 3. The logarithmic part of $F(n)$ for the TFI model. $F(n, L)$ was computed for $L = 2, 4, \cdots 40$, and $\gamma(n)$ extracted by the same procedure as for the XXZ model. The dashed lines are $\gamma(n) = -\frac{1}{8}n$ and $\gamma(n) = \frac{3}{8}n$. In the inset, the data is collapsed by plotting $\gamma(n)/n$ as a function of $(n-1)\gamma'(1)$.

the logarithmic terms are compactification-independent while the $O(1)$ terms, arising from both sectors, are not.

The $c = 1/2$ Ising model exhibits strikingly different behavior from the compact boson. In the transfer matrix formalism, it is sufficient to consider the Shannon entropy of the critical transverse-field Ising model,

$$H = -\sum_{i=1}^{N-1} \sigma_i^z \sigma_{i+1}^z + \sum_{i=1}^{N} \sigma_i^x \tag{11}$$

The Shannon entropy is calculated in the σ^z basis.

The extracted logarithm $\gamma(n)$, shown in Fig. 3, suggests a discontinuous n-dependence at $n = 1$. The dashed lines illustrate the likely convergence to

$$\gamma(n) = \begin{cases} -\frac{1}{8}n & \text{for } n < 1 \\ 0 & \text{for } n = 1 \\ \frac{3}{8}n & \text{for } n > 1 \end{cases} . \tag{12}$$

Note that the rotation used in the boson case predicts that $\gamma(n) \propto (n-1)$, as there is always one 'free' center of mass field. In the present Ising case, $\gamma(n) \propto n$, which is evidence that the rotation trick is not applicable and a new analysis is required. In the inset of Fig. 3, the data is collapsed by plotting $\gamma(n)/n$ as a function of $\gamma'(1)(n-1)$. Recall $\gamma(1) = 0$ identically due to the normalization of the entanglement spectrum.

The large and small n limits can be understood as follows. At large n, $\mathcal{Z}(n)$ is dominated by the probability $p_\uparrow = |\langle \uparrow\uparrow \cdots | 0 \rangle|^2$ and its partner $p_\downarrow$. In this 'low temperature' regime, the defect line at $\tau = 0$ is asymptotically a 'fixed' defect line. Now all n fields experience this fixed defect condition, not $n-1$ of them, and

$$F(n) \sim n(F_\uparrow - F) - \log(2) \tag{13}$$

Here $F_\uparrow$ is the free energy of a *single* replica with spins constrained to $\sigma = +1$ along the defect. Again, there is an anomaly due to the 'cut strip' geometry. The external boundary conditions are free, so the relevant scaling dimension is $h_{f\uparrow} = \frac{1}{16}$ [21]. Using Eq. (10), $\gamma(n) = \frac{3}{8}n$ as observed. Likewise, in the small n limit, the defect becomes disordered. This is obvious at the $n = 1/2$ point, where the geometry is in fact a half-strip with a free boundary at $\tau = 0$. With $h_{ff} = 0$, we arrive at $\gamma(n) = -\frac{1}{8}n$ as observed. While these results strictly apply only in large and small n limits, the data appears to support an n-dependent phase transition: for $n < 1$, the defect flows to free boundary conditions for $2n$ decoupled half strips, while for $n > 1$, the defect is fixed. This interpretation is consistent with numerical results for the $O(1)$ term on a cylinder[16]. The renormalization group equations for these b.c. flows can be analyzed perturbatively [22], and support the hypothesis of a phase transition. This perturbative approach could be generalized to other CFTs in order to study further possible entanglement boundary conditions and replica transitions.

The authors acknowledge conversations with I. Affleck, J. Cardy, E. Fradkin, A. Ludwig and M. Oshikawa, and support from DOE DE-AC02-05CH11231 (JHB) and NSF DMR-0804413 (JEM).

[1] C. Holzhey, F. Larsen, and F. Wilczek, Nucl. Phys. B, **424**, 443 (1994).
[2] G. Vidal, J. I. Latorre, E. Rico, and A. Kitaev, Phys. Rev. Lett., **90**, 227902 (2003); P. Calabrese and J. Cardy, J. Stat. Mech., **06**, P06002 (2004).
[3] G. Refael and J. E. Moore, Phys. Rev. Lett., **93**, 260602 (2004); N. Laflorencie, Phys. Rev. B, **72**, 140408 (2005); R. Santachiara, J. Stat. Mech., L06002 (2006).
[4] P. Calabrese and A. Lefevre, Phys. Rev. A, **78**, 32329 (2008); M. Fagotti, P. Calabrese, and J. E. Moore, Phys. Rev. B, **83**, 045110 (2011).
[5] X. Chen, Z.-C. Gu, and X.-G. Wen, Phys. Rev. B, **83**, 035107 (2011).
[6] F. Pollmann, S. Mukerjee, A. Turner, and J. E. Moore, Phys. Rev. Lett., **102**, 255701 (2009).
[7] S. Ryu and T. Takayanagi, Phys. Rev. Lett., **96**, 181602 (2006).
[8] M. A. Metlitski, C. A. Fuertes, and S. Sachdev, Phys. Rev. B, **80**, 115122 (2009).
[9] L. Tagliocozzo, G. Evenbly, and G. Vidal, Phys. Rev. B, **80**, 235127 (2009).
[10] E. Ardonne, P. Fendley, and E. Fradkin, Ann. Phys., **310**, 493 (2004); S. V. Isakov, P. Fendley, A. W. W. Ludwig, S. Trebst, and M. Troyer, Phys. Rev. B, **83**, 125114 (2011).
[11] D. S. Rokhsar and S. A. Kivelson, Phys. Rev. Lett., **61**, 2376 (1988).
[12] E. Fradkin and J. E. Moore, Phys. Rev. Lett., **97**, 050404 (2006).
[13] J.-M. Stéphan, S. Furukawa, G. Misguich, and V. Pasquier, Phys. Rev. B, **80**, 184421 (2009).
[14] B. Hsu and E. Fradkin, J. Stat. Mech.: Theor. Exp., **2010**, P09004 (2010).

[15] M. Oshikawa, arXiv:1007.3739v1.
[16] J.-M. Stéphan, G. Misguich, and V. Pasquier, Phys. Rev. B, **82**, 125455 (2010).
[17] G. Vidal, Phys. Rev. Lett., **91**, 147902 (2003).
[18] J.-M. Stéphan, G. Misguich, and V. Pasquier, arXiv:1104.2544.
[19] I. Affleck, J. Phys. A: Math. Gen., **31**, 2761 (1998).
[20] J. L. Cardy and I. Peschel, Nucl. Phys. B, **300**, 377 (1988).
[21] J. L. Cardy, Nucl. Phys. B, **324**, 581 (1989).
[22] J. L. Cardy, J. Phys. A: Math. Gen., **24**, L1315 (1991).